The distribution and ultrastructure of the forming blood capillaries and the effect of apoptosis on vascularization in mouse embryonic molar mesenchyme

Guohua Yuan,
Key Laboratory of Oral Biomedicine of Ministry of Education, School & Hospital of Stomatology, Wuhan University, Wuhan, Hubei, People's Republic of China 430079

Li Zhang,
Key Laboratory of Oral Biomedicine of Ministry of Education, School & Hospital of Stomatology, Wuhan University, Wuhan, Hubei, People's Republic of China 430079

Guobin Yang,
Key Laboratory of Oral Biomedicine of Ministry of Education, School & Hospital of Stomatology, Wuhan University, Wuhan, Hubei, People's Republic of China 430079

Jingwen Yang,
Key Laboratory of Oral Biomedicine of Ministry of Education, School & Hospital of Stomatology, Wuhan University, Wuhan, Hubei, People's Republic of China 430079

Chunyan Wan,
Key Laboratory of Oral Biomedicine of Ministry of Education, School & Hospital of Stomatology, Wuhan University, Wuhan, Hubei, People's Republic of China 430079

Lu Zhang,
Key Laboratory of Oral Biomedicine of Ministry of Education, School & Hospital of Stomatology, Wuhan University, Wuhan, Hubei, People's Republic of China 430079

Guangtai Song,
Key Laboratory of Oral Biomedicine of Ministry of Education, School & Hospital of Stomatology, Wuhan University, Wuhan, Hubei, People's Republic of China 430079

Shuo Chen, and
Department of Developmental Dentistry, The University of Texas Health Science Center at San Antonio, San Antonio, TX 78229-3900, USA

Zhi Chen
Key Laboratory of Oral Biomedicine of Ministry of Education, School & Hospital of Stomatology, Wuhan University, Wuhan, Hubei, People's Republic of China 430079

Shuo Chen: chens0@uthscsa.edu; Zhi Chen: zhichen@whu.edu.cn

Abstract

Vascularization is essential for organ and tissue development. Teeth develop through interactions between epithelium and mesenchyme. The developing capillaries in the enamel organ, the dental

epithelial structure, occur simultaneously by mechanisms of vasculogenesis and angiogenesis at the onset of dentinogenesis. The vascular neoformation in the dental mesenchyme has been reported to start from the cap stage. However, the mechanisms of vascularization in the dental mesenchyme remain unknown. In the hope of understanding the mechanisms of the formation of dental mesenchymal vasculature, mouse lower molar germs from embryonic day (E) 13.5 to E16.5 were processed for immunostaining of CD31 and CD34, terminal deoxynucleotidyltransferase-mediated dUTP-biotin nick end labeling (TUNEL) and transmission electron microscopy (TEM). In addition, the role of apoptosis for the vascularization in dental mesenchyme was examined by in vitro culture of E14.0 lower molars in the presence of the apoptosis inhibitor (z-VAD-fmk) and a subsequent subrenal culture. Our results showed that CD31- and CD34-positive cells progressively entered the central part of the dental papilla from the peridental mesenchyme. For TEM, angioblasts, young capillaries with thick endothelium and endothelial cells containing vacuoles were observed in peripheral dental mesenchyme, suggesting vasculogenesis was taking place. The presence of lateral sprouting, cytoplasmic filopodia and transluminal bridges in the dental papilla suggested angiogenesis was also occurring. Inhibition of apoptosis delayed the angiogenic vascularization of the dental papilla. Therefore, these data demonstrated that molar mesenchyme is progressively vascularized by mechanisms of both vasculogenesis and angiogenesis and apoptosis partially contributes to the vascularization of the dental papilla.

Keywords

Apoptosis; Angiogenesis; Electron microscopy; Tooth mesenchyme; Vasculogenesis

Introduction

Vascularization is essential for organ and tissue development. The vasculature is required for maintaining metabolic homeostasis by supplying oxygen and nutrients as well as excreting metabolized products (Corpron et al. 1976; Arfuso 2006). To date, it has been known that neovascularization of the embryonic organs occurs by vasculogenesis or angiogenesis or both (Patan 2000; Maina 2004). Vasculogenesis is an in situ process by which progenitor cells differentiate and give rise to capillaries (Patan 2000; Ratajska et al. 2006), while angiogenesis refers to the formation of new capillaries from pre-existing ones, comprising endothelial sprouting and intussusceptive microvascular growth (IMG). The sprouting process is based on endothelial cell migration, proliferation and tube formation, while IMG divides existing vessel lumens by formation and insertion of cell bridges and folds of interstitial tissue into the vessel lumen (Djonov et al. 2000; Patan 2000). Both vasculogenesis and angiogenesis exhibit characteristic structural features using transmission electron microscope (Maina 2004; Manzke et al. 2005; Arfuso 2006; Quagliata et al. 2008).

Teeth develop as a result of sequential and reciprocal interactions between epithelium and cranial neural crest-derived mesenchyme (Peterková et al. 2003; Zhang et al. 2005). The vascularization of the enamel organ, the dental epithelial structure, occurs at the onset of dentinogenesis. Analysis of the ultrastructural features showed that both vasculogenesis and angiogenesis were involved in the neoformation of capillaries in the dental epithelium (Tsuzuki and Sasa 1994; Manzke et al. 2005). For the dental mesenchyme, a recent study showed that blood vessels form between embryonic day (E) 14 and E16, the stage when the enamel knot (EK) is clearly visible (Nait Lechguer et al. 2008). However, to our knowledge, the ultrastructural features of neovascularization in the embryonic dental mesenchyme have not been described. It is still not clear that the formation of vascular networks in the dental mesenchyme is established by vasculogenesis and/or angiogenesis.

Apoptosis, also called programmed cell death, takes part in both morphogenesis of embryonic tissues and regulation of adult tissue homeostasis (Peterková et al. 2003; Matalova et al. 2004). Besides, apoptosis has been demonstrated to participate in the very early stages of vasculogenesis and angiogenesis in the human placenta (Tertemiz et al. 2005); apoptotic cells have been reported to initiate the formation of directional endothelial cell sprouts towards them in cell culture (Weihua et al. 2005). Apoptosis accompanies the entire development of teeth. The most evident apoptosis in molar development occurs in the EK at E14.5 (Peterková et al. 2003; Matalova et al. 2004). The concurrence of apoptosis in the EK and invasion of blood vessels toward dental mesenchyme underlying the EK made us postulate that the apoptosis of the EK may contribute to the vascularization of mouse molar mesenchyme.

In the present study, we investigate spatiotemporal and morphologic patterns of vascularization of mouse molar mesenchyme from E13.5 to E16.5, using immunostaining and transmission electron microscopy (TEM). We also examine the role of apoptosis for vascularization in the molar mesenchyme by using a caspase inhibitor, z-VAD-fmk, concomitant with in vitro organ culture and tooth germ transplantation into kidney capsules.

Materials and methods

Generation of embryos

The protocol of animal use was approved by the Animal Welfare Committee of the School and Hospital of Stomatology at Wuhan University. The ICR mice (*Mus musculus*) were mated overnight. Noon of the day on which vaginal plugs were detected was considered as E0.5 (Yuan et al. 2008). Three embryos for each time point were sacrificed and taken for each of the following analyses.

Histology, immunostaining of CD34 and CD31 and TUNEL assay

The embryonic mouse heads from E13.5 to E16.5 were harvested and made into serial frontal sections, which were then deparaffinated with xylene and rehydrated with a series of ethanol. Some of the sections were stained with hematoxylin and eosin (H&E) for histology.

To identify the distribution of forming vasculature and VEGF in mouse molar germs, two anti-CD34 antibodies (goat polyclonal IgG, Santa Cruz Biotechnology, CA, USA and rabbit monoclonal IgG, Abcam, Cambridge, USA), anti-CD31 antibody (goat polyclonal IgG; R&D) and anti-VEGF antibody (rabbit polyclonal IgG; Santa Cruz Biotechnology) were used as first antibodies for immunohistochemistry and double immunofluorescence. Briefly, for immunohistochemistry, the rehydrated tissue sections were incubated in 3 % H_2O_2 to remove the endogenous peroxidase activity. For antigen retrieval, the slides were immersed in 0.01 M citrate buffer and microwaved in a steamer. After treatment with 10 % normal rabbit or goat serum to block non-specific binding, the sections were incubated with goat anti-CD31 or goat anti-CD34 or rabbit anti-VEGF antibody at 4 °C overnight. Those sections incubated with control IgG (Santa Cruz Biotechnology) instead of first antibody were set as control. Then, the sections were incubated with biotinylated secondary antibody solution (Vector Laboratories, Burlingame, CA, USA) and Vectastain Elite ABC reagent (Vector Laboratories). Subsequently, the tissue sections were stained with DAB and counterstained with Mayer's hematoxylin. For double immunofluorescence, the sections were washed in phosphate-buffered saline (PBS) and blocked with 10 % donkey serum in PBS for 30 min prior to being incubated with rabbit anti-CD34 and goat anti-CD31 antibodies at 4 °C overnight, which were recognized by a donkey anti-rabbit secondary antibody conjugated with Alexa Fluo® 488 (Invitrogen Life technologies, USA) and a donkey anti-goat secondary antibody conjugated with Alexa Fluo® 568 (Invitrogen).

Apoptosis was detected by a terminal deoxynucleotidyltransferase-mediated dUTP-biotin nick end labeling (TUNEL) assay using the In Situ Cell Death Detection kit (fluorescein) (Roche) according to the manufacturer's instructions. Briefly, the rehydrated sections were treated with proteinase K at 37 °C for 15 min and incubated with substrate reaction at 37 °C for 60 min. Then, the slides were mounted and observed under a fluorescent microscope. A negative control incubated without the terminal deoxynucleotidyl transferase showed no fluorescent signal (data not shown).

TEM of the vasculature in mouse molar mesenchyme from E13.5 to E16.5

Mouse mandibles from E13.5 to E16.5 were dissected in cold PBS. The molar germs were immediately harvested with fine forceps under a stereomicroscope and immersed in a mixture of 4 % glutaraldehyde and 4 % paraformaldehyde in 0.1 M sodium cacodylate (pH 7.4) at 4 °C. The specimens were postfixed in a solution of 1 % osmium tetroxide in 0.1 M sodium cacodylate (pH 7.4). Then the tissues were dehydrated through a series of ethanol in increasing concentrations, cleared in acetone and embedded in Epon 812. Ultrathin sections were cut with diamond knives on an LKB-V ultratome and double-stained with uranyl acetate and lead citrate. The sections were examined under a transmission electron microscope. Images of the blood vessels in the dental mesenchyme were taken and analyzed (ESM Fig. S1a, d, g, j; areas surrounded by the dashed lines).

Apoptosis inhibition and transplantation into kidney capsules

E14.0 molar tooth germs were dissected from the lower jaw in cold PBS and cultured by Trowell's culture method (Yuan et al. 2008). In the experimental cases, the media were supplemented with the specific caspase inhibitor z-VAD-fmk (MBL International, Japan) at a concentration of 50, 100 μM from the beginning of the culture. In the control cases, 1 % DMSO was used to monitor any DMSO-related effects. After in vitro culture for 2 days, the tooth germs were transplanted to mouse kidney capsules as described previously and cultured for another 2 or 4 days (Yuan et al. 2008). Then the molar tissues were processed for the H&E staining, immunohistochemistry of CD31, and TUNEL assay as described above.

Results

Distribution and ultrastructure of the capillaries in molar mesenchyme from E13.5 to E16.5

To localize the forming vasculature in mouse molar mesenchyme before it could be distinguished under routine histological staining, CD31 and CD34 expression in the mouse molar germs from E13.5 to E16.5 was performed using double immunofluorescence and immunohistochemistry. Staining of CD31 and CD34 was negative in the dental epithelium during bud stage to early bell stage (Fig. 1; ESM Fig. S1). Control slides, which were incubated with rabbit IgG (ESM Fig. S1m) or goat IgG (ESM Fig. S1n) instead of first antibodies, showed a negative reaction, confirming the specificity of the antibodies used in this study. Meanwhile, a TUNEL assay was performed to show the spatial relationship between apoptotic cells and vasculature during this period (Fig. 1).

To analyze the cellular mechanism of vascularization in mouse molar mesenchyme, TEM was performed in CD31-and CD34-positive areas surrounded by the dashed lines (ESM Fig. S1a, d, g, j). Our images showed that abundant free ribosomes, mitochondria, rough endoplasmic reticulum (RER), Golgi complexes and pinocytic vesicles were present in angioblasts and endothelial cells. Most endothelial cells had irregular thickness. The basal laminas of most capillaries were discontinuous or absent. Figures 2 and 3 are representative TEM images.

E13.5 (Bud stage)—At E13.5, the molar epithelium has invaginated into the mesenchyme to form an epithelial bud, accompanied with localized condensation of the underlying mesenchyme (ESM Fig. S1a). CD31- and CD34-positive cells appeared around the condensed mesenchyme. Some positive cells did not show a definite lumen on sections. Some of them were tubular and formed the first capillaries (Fig. 1a–d; ESM Fig. S1b, c). Apoptotic cells were shown in the surface and tip of the epithelial bud (Fig. 1e).

For TEM, most of these first capillaries in the dental mesenchyme had an exiguous lumen, where the erythrocytes and endothelial cells adapted their shapes reciprocally. Short cytoplasmic processes from the neighboring mesenchymal cells were in close spatial relationship to or occasionally contacted the abluminal surface of the capillaries (Fig. 2a).

E14.5 (Early cap stage)—At E14.5, molar epithelium took the form of a cap configuration with an EK located in the center, while molar mesenchyme developed into the dental papilla and dental follicle (ESM Fig. S1d). CD31- and CD34-positive cells were detected in the dental follicle and in the mandibular portion of the dental papilla where some positive cells appeared to be directed toward the central part of the papilla (Fig. 1f–i; ESM Fig. S1e, f). Apoptotic cells were clearly visible in the EK (Fig. 1j).

In the dental follicle, angioblasts with large nuclei and characteristic conspicuous cytoplasmic processes were visualized. Some of the angioblasts connected end by end to each other, resulting in primitive vascular lumen formation (Fig. 2b). Cytoplasmic vacuoles were seen in a forming endothelial cell. A nucleated erythrocyte was surrounded by newly forming endothelial cells (Fig. 2c, f). An immature microvascular tube consisting of a few layers of cells in an onion shape was also observed in the dental follicle. The capillary had a relatively thick wall with an exiguous lumen, in which an apoptotic cell with electron-dense cytoplasm, a few recognizable degenerate mitochondria and a collection of glycogen were discernible. An angioblast-like cell adhered to the wall of the microvascular tube through filopodia extensions (Fig. 2d) and small intercellular spaces were present between the neighboring endothelial cell and angioblast-like cell (Fig. 2e). Meanwhile, in the lower part of the dental mesenchyme, capillaries showing lateral sprouting toward the central dental papilla were observed. The sprouting endothelial cells were rich in filopodia. The intercellular space between the endothelial cell and pericyte-like cell was irregular (Fig. 2g). Some capillaries contained apoptotic bodies inside their lumen (Fig. 2h).

E15.5 (late cap stage)—At E15.5, the molar germ developed into the late cap stage (ESM Fig. S1g). CD31- and CD34-positive cells were detected in the central part of the dental papilla. Some of the positive cells were in close proximity to the presumptive odontoblasts (Fig. 1k–n, ESM Fig. S1h, i). Apoptotic cells were found in the residual EK and dental lamina (Fig. 1o).

For TEM, in addition to the phenomena observed at E14.5, capillaries containing erythrocytes and apoptotic bodies, as well as monocytes, were seen. Pinocytic vesicles were seen under the luminal cytoplasm. Abluminal protrusions of the endothelial cells were apparent and at some points made contact with the adjacent cells (Fig. 3a). Some other capillaries showed cytoplasmic filopodia at the luminal side rising toward the opposite side. Once the cytoplasmic filopodia reached the opposite side, the pre-existing capillary was split into two vascular units (Fig. 3b). A pericyte-like cell containing cytoplasmic vacuolar spaces adhered to the abluminal surface of the capillary (Fig. 3b, c).

E16.5 (early bell stage)—By E16.5, the molar started to reach the bell stage (ESM Fig. S1j). CD31- and CD34-positive cells were visualized in the dental papilla in an orientation toward the presumptive odontoblasts on the future cusp positions (Fig. 1p–s; ESM Fig. S1k,

l). Apoptotic cells are detected in secondary EKs with sporatic distribution in the dental follicle, outer enamel epithelium and stellate reticulum (Fig. 1t).

Under TEM, further processes of capillary formation were observed involving laminar extensions of the endothelial cells protruding into the lumen of pre-existing capillaries. Cytoplasmic transluminal bridges formed (Fig. 3d–f), which sometimes included the nuclear area (Fig. 3e, f) and split the capillary lumen into two compartments.

Vascularization of molar mesenchyme was delayed after z-VAD-fmk treatment

To investigate whether apoptosis of EK functions during molar mesenchymal vascularization, dissected mouse molars at E14.0 were cultured in vitro with z-VAD-fmk at a concentration of 0, 50, or 100 μM for 2 days, then transplanted to mouse kidney capsules for another 2- or 4-day subrenal culture. To confirm the apoptosis inhibition efficiency of z-VAD-fmk, a TUNEL assay was performed. Apoptotic cells were present in the control but absent in the z-VAD-fmk treated specimens (ESM Fig. S2). To observe the vascularization of the cultured tooth germs, CD31 immunohistochemistry was conducted. After Trowell organ culture for 2 days with or without z-VAD-fmk, no CD31-positive cells were observed in the central part of the dental papilla (Fig. 4j; data not shown). After a following subrenal culture for 2 days, CD31-positive blood vessels have invaded the central dental papilla area in control molars (Fig. 4a–c). However, in molars treated with z-VAD-fmk at a concentration of 50 or 100 μM, no blood vessels existed in the central part of the molar papilla after 2-day subrenal culture (Fig. 4d–i). However, after 4-day subrenal culture, blood vessels were clearly visible in the central part of the dental papilla treated with 50 (Fig. 4k) or 100 μM z-VAD-fmk (Fig. 4l).

Localization of VEGF in tooth germs

VEGF plays a pivotal role in the regulation of angiogenesis (Carmeliet et al. 1996; Ferrara et al. 1996). Immunohistochemistry of VEGF was carried out at E13.5 and E16.5. At E13.5, VEGF is expressed in both dental epithelium and dental mesenchyme. At E16.5, VEGF is localized in the dental papilla, inner enamel epithelium, stellate reticulum and outer enamel epithelium of the tooth germ (ESM Fig. S3).

Discussion

In the present study, to determine the mechanisms of vascularization in mouse dental mesenchyme, we first performed immunostaining of CD31 and CD34 in mouse molars from E13.5 to E16.5 and, second, observed the ultrastructural characteristics of the vasculature in molar mesenchyme at the same stages. Lastly, we analyzed the possible contribution of apoptosis in the EK to vascularization in the dental papilla using the apoptosis inhibitor z-VAD-fmk. Our results demonstrated that molar mesenchyme is progressively vascularized by mechanisms of both vasculogenesis and angiogenesis during the period investigated and apoptosis partially contributes to vascularization of molar mesenchyme.

In this study, immunostaining of CD31 and CD34, two well-recognized vasculature markers, were used to identify the vascularization of mouse molar mesenchyme. CD31 is a platelet-derived cell adhesion factor. Hematopoietic progenitor cells, branching angiogenic areas and microvessel connecting tubes are positive for CD31 (Tertemiz et al. 2005; Ribatti 2007). In addition, CD31 is a marker of mature endothelium (Nagatsuka et al. 2005; Ribatti 2007). CD34 is a transmembranous sialo protein. It is intensely expressed by hemangioblastic cells, hematopoietic stem cells, undifferentiated vascular endothelial cells and immature endothelial cells, as well as microvessels with strong remodeling activity. In contrast, well-established endothelial cells and differentiated hematopoietic cells are CD34-

negative (Fina et al. 1990; Cheng et al. 1996; Asahara et al. 1997; Trubiani et al. 2003; Demir et al. 2004; Nagatsuka et al. 2005; Tertemiz et al. 2005; Ratajska et al. 2006; Ribatti 2007). Immunostaining results showed that, at E13.5 and E14.5, CD31- and CD34-positive cells were mainly distributed in peripheral mesenchyme (Fig. 1a–d, f–i, ESM Fig. S1a–f). From E15.5 to E16.5, the CD34- and CD31-positive cells progressively appeared in the central part of the dental papilla. Some of these positive cells even reached up to the future odontoblasts (Fig. 1k–n, p–s; ESM Fig. S1g–l). Mouse dental vascularization at E14 and at E16 was reported using CD31 and VEGFR2 immunostaining (Nait Lechguer et al. 2008; Rothová et al. 2011), which was consistent with our results of CD31 and CD34 immunostaining. Double immunofluorescence results showed that CD31- and CD34-positive cells completely overlapped (Fig. 1), implying that all the blood vessels in molar germs were immature during the period investigated.

To observe whether vascularization in mouse molar mesenchyme involves vasculogenesis and/or angiogenesis, TEM was carried out from E13.5 to E16.5. To our knowledge, this study would appear to be the first description of ultrastructural characteristics of neovascularization in early mouse molar mesenchyme. Abundant ribosomes, mitochondria, RER and Golgi complexes in endothelial cytoplasms demonstrated morphologically that endothelial cells were actively involved in protein synthesis. Cytoplasmic protrusions directed toward the luminal or abluminal spaces (Figs. 2g; 3a, d–f), thick capillary walls (Fig. 2d) and pinocytic vesicles were characteristics of immature or remodeling endothelial cells (Tsuzuki and Sasa 1994; Okada and Aharinejad 1997; Quagliata et al. 2008).

The cellular mechanisms of vascularization in mouse molar mesenchyme can be described as follows. On the one hand, our images suggested that vascularization of molar peripheral mesenchyme (dental follicle) takes place by the mechanism of vasculogenesis (Fig. 2b–f). Angioblasts were found with characteristic filopodial extensions and large nuclei (Fig. 2b, c) (Maina 2004; Quagliata et al. 2008). Some angioblasts interconnected across minute junctions and formed the primitive capillary lumen (Fig. 2b, c) (Quagliata et al. 2008). A NRBC belonging to late erythroblastic stages of differentiation (a halo around a nucleus indicated the commencement of the nucleus shedding) (Ratajska et al. 2006) was seen (Fig. 2c, f). NRBCs may be a source of certain paracrine substances to the adjacent cells (angioblasts) in vasculogenesis (Maina 2004). Nascent blood vessels developing from blood island-like structures were also observed. These blood vessels showed thick endothelium and a narrow lumen (Fig. 2d; Quagliata et al. 2008). Apoptosis contributed to this stage of vasculogenesis from blood island-like structures (Fig. 2d), similar to that observed in the human placenta (Tertemiz et al. 2005). Intercellular spaces between the endothelial cells and angioblasts (Fig. 2e) and the vacuolization of endothelial cytoplasm (Fig. 2c, f) were visualized and they might contribute to lumenization during subsequent development (Manzke et al. 2005; Tertemiz et al. 2005). On the other hand, morphometric evaluation of vasculature in the dental papilla revealed that angiogenesis also took part in vascularization of molar mesenchyme (Fig. 2g). Loss of basal lamina, the presence of lateral sprouting and the presence of cytoplasmic filopodia (Fig. 2g) indicated that sprouting angiogenesis was actively occurring and penetrating the tooth papilla (Maina 2004; Manzke et al. 2005; Quagliata et al. 2008). At more advanced developmental stages, luminal cytoplasmic filopodia were sent out to reach the opposite ones (Fig. 3b) and formed cytoplasmic transluminal bridges (Fig. 3d–f) that split the lumen of existent capillaries. These phenomena indicated that non-sprouting angiogenesis was also taking place and led to an increase in the vascular unit number through the division of pre-existing ones (Djonov et al. 2000; Demir et al. 2004; Manzke et al. 2005). Based on our observations, this indicates that vasculogenesis and angiogenesis occurred simultaneously during vascularization of molar mesenchyme from E13.5 to E16.5. Previous studies found host cells contributed to the

vascularization of transplanted molars (Nait Lechguer et al. 2008), which also suggests that angiogenesis is involved in tooth vascular network development.

Irregular spaces between endothelial cells and pericyte-like cells (Fig. 2g) and the presence of vacuoles within the pericyte-like cell cytoplasm (Fig. 3c) were depicted. These pericyte-like cells may participate in angiogenesis as reported previously (Ozerdem and Stallcup 2003; Arfuso 2006).

Previous studies have demonstrated that apoptosis is involved in the elimination of diastemal tooth germs and the shaping and size of functional tooth germs (Coin et al. 2000; Peterková et al. 2003; Matalova et al. 2004; Kim et al. 2006). The distribution pattern of TUNEL-positive cells (Fig. 1) in this study is consistent with previous reports (Peterková et al. 2003; Matalova et al. 2004). Dental apoptosis is caspase-dependent. A specific caspase inhibitor, z-VAD-fmk, has been used and successfully abrogated the apoptosis in tooth germs in previous reports (Coin et al. 2000; Kim et al. 2006). In this study, inhibition of the apoptosis in the EK by z-VAD-fmk delayed the vascularization of the dental papilla (Fig. 4a–h), suggesting that apoptosis in the EK likely contributes to the directional angiogenic sprouting of the blood vessels from the surrounding dental mesenchyme to the central part of the dental papilla. Interestingly, in the dental epithelium, a concurrence of involution of the stellate reticulum by apoptosis with the vascularization of the enamel organ has also been found previously (Baratella et al. 1999; Manzke et al. 2005). The mechanism of apoptotic cells initiating endothelial cell sprouting toward them was found to be dependent of the negative charges on the apoptotic cell surface but independent of diffusible molecules (Weihua et al. 2005). Electrical stimulation induces significant angiogenesis in vivo and in vitro and endogenous electric fields are widespread (Kanno et al. 1999; Bai et al. 2004). Further investigations are necessary to test whether apoptotic EK cells attract endothelial sprouting by expression of negative charges and/or formation of an endogenous electric field. Meanwhile, the vascularization of the dental papilla also critically depends on diffusible molecules, such as VEGF expressed in tooth germs (ESM Fig. S3; Aida et al. 2005; Ide et al. 2011; Miwa et al. 2008). In addition, Shh protein has been found to guide angiogenesis and vasculogenesis in various tissues (reviewed by Fuchs et al. 2012) and the downregulation of Shh expression was found to be delayed after apoptosis inhibition (Coin et al. 2000), so the persistent Shh may promote the vascularization seen in the experimental group. The expression of VEGF and persistent Shh may explain the vascularization of the dental papilla after 4-day subrenal culture in tooth germs treated with apoptosis inhibitor (Fig. 4k, l).

In conclusion, at E13.5 and E14.5, primitive endothelia differentiate around the tooth bud and form the initial lumen, while after E14.5, endothelial tubes in the lower part of the molar mesenchyme elongate and branch toward the central dental papilla. Apoptosis of the EK partly contributes to the invasion of blood vessels into the dental papilla. Further investigations are needed to determine the mechanism by which apoptosis promotes angiogenesis and to provide deeper insights into the vascularization of molar mesenchyme.

Supplementary Material

Refer to Web version on PubMed Central for supplementary material.

Acknowledgments

References

Aida M, Irié T, Aida T, Tachikawa T. Expression of protein kinases C betaI, betaII, and VEGF during the differentiation of enamel epithelium in tooth development. J Dent Res. 2005; 84:234–239. [PubMed: 15723862]

Arfuso F. A study of physiologic angiogenesis in the human using the dental pulp as an in vivo model. Endothelium. 2006; 13:359–363. [PubMed: 17090409]

Asahara T, Murohara T, Sullivan A, Silver M, van der Zee R, Li T, Witzenbichler B, Schatteman G, Isner JM. Isolation of putative progenitor endothelial cells for angiogenesis. Science. 1997; 275:964–967. [PubMed: 9020076]

Bai H, McCaig CD, Forrester JV, Zhao M. DC electric fields induce distinct preangiogenic responses in microvascular and macrovascular cells. Arterioscler Thromb Vasc Biol. 2004; 24:1234–1239. [PubMed: 15130919]

Baratella L, Arana-Chavez VE, Katchburian E. Apoptosis in the early involuting stellate reticulum of rat molar tooth germs. Anat Embryol (Berl). 1999; 200:49–54. [PubMed: 10395005]

Carmeliet P, Ferreira V, Breier G, Pollefeyt S, Kieckens L, Gertsenstein M, Fahrig M, Vandenhoeck A, Harpal K, Eberhardt C, Declercq C, Pawling J, Moons L, Collen D, Risau W, Nagy A. Abnormal blood vessel developement and lethality in embryos lacking a single VEGF allele. Nature. 1996; 380:435–439. [PubMed: 8602241]

Cheng J, Baumhueter S, Cacalano G, Carver-Moore K, Thibodeaux H, Thomas R, Broxmeyer HE, Cooper S, Hague N, Moore M, Lasky LA. Hematopoietic defects in mice lacking the sialomucin CD34. Blood. 1996; 87:479–490. [PubMed: 8555469]

Coin R, Kieffer S, Lesot H, Vonesch JL, Ruch JV. Inhibition of apoptosis in the primary enamel knot does not affect specific tooth crown morphogenesis in the mouse. Int J Dev Biol. 2000; 44:389–396. [PubMed: 10949048]

Corpron RE, Avery JK, Morawa AP, Lee SD. Ultrastructure of capillaries in mouse periodontium. J Dent Res. 1976; 55:551. [PubMed: 1063767]

Demir R, Kayisli UA, Seval Y, Celik-Ozenci C, Korgun ET, Demir-Weusten AY, Huppertz B. Sequential expression of VEGF and its receptors in human placental villi during very early pregnancy: differences between placental vasculogenesis and angiogenesis. Placenta. 2004; 25:560–572. [PubMed: 15135240]

Djonov V, Schmid M, Tschanz SA, Burri PH. Intussusceptive angiogenesis: its role in embryonic vascular network formation. Circ Res. 2000; 86:286–292. [PubMed: 10679480]

Ferrara N, Carver-Moore K, Chen H, Dowd M, Lu L, O'Shea KS, Powell-Braxton L, Hillan KJ, Moore MW. Heterozygous embryonic lethality induced by targeted inactivation of the VEGF gene. Nature. 1996; 380:439–442. [PubMed: 8602242]

Fina L, Molgaard HV, Robertson D, Bradley NJ, Monaghan P, Delia D, Sutherland DR, Baker MA, Greaves MF. Expression of the CD34 gene in vascular endothelial cells. Blood. 1990; 75:2417–2426. [PubMed: 1693532]

Fuchs S, Dohle E, Kirkpatrick CJ. Sonic Hedgehog-mediated synergistic effects guiding angiogenesis and osteogenesis. Vitam Horm. 2012; 88:491–506. [PubMed: 22391318]

Ide S, Tokuyama R, Davaadorj P, Shimozuma M, Kumasaka S, Tatehara S, Satomura K. Leptin and vascular endothelial growth factor regulate angiogenesis in tooth germs. Histochem Cell Bio. 2011; 135:281–292. [PubMed: 21340571]

Kanno S, Oda N, Abe M, Saito S, Hori K, Handa Y, Tabayashi K, Sato Y. Establishment of a simple and practical procedure applicable to therapeutic angiogenesis. Circulation. 1999; 99:2682–2687. [PubMed: 10338463]

Kim JY, Cha YG, Cho SW, Kim EJ, Lee MJ, Lee JM, Cai J, Ohshima H, Jung HS. Inhibition of apoptosis in early tooth development alters tooth shape and size. J Dent Res. 2006; 85:530–535. [PubMed: 16723650]

Maina JN. Systematic analysis of hematopoietic, vasculogenetic, and angiogenetic phases in the developing embryonic avian lung, Gallus gallus variant domesticus. Tissue Cell. 2004; 36:307–322. [PubMed: 15385148]

Manzke E, Katchburian E, Faria FP, Freymuller E. Structural features of forming and developing blood capillaries of the enamel organ of rat molar tooth germs observed by light and electron microscopy. J Morphol. 2005; 265:335–342. [PubMed: 16094655]

Matalova E, Tucker AS, Sharpe PT. Death in the life of a tooth. J Dent Res. 2004; 83:11–16. [PubMed: 14691106]

Miwa Y, Fujita T, Sunohara M, Sato I. Immunocytochemical localization of vascular endothelial growth factor and vascular endothelial growth factor receptor-2 of the human deciduous molar tooth germ development in the human fetus. Ann Anat. 2008; 190:246–251. [PubMed: 18396391]

Nagatsuka H, Hibi K, Gunduz M, Tsujigiwa H, Tamamura R, Sugahara T, Sasaki A, Nagai N. Various immunostaining patterns of CD31, CD34 and endoglin and their relationship with lymph node metastasis in oral squamous cell carcinomas. J Oral Pathol Med. 2005; 34:70–76. [PubMed: 15641985]

Nait Lechguer A, Kuchler-Bopp S, Hu B, Haikel Y, Lesot H. Vascularization of engineered teeth. J Dent Res. 2008; 87:1138–1143. [PubMed: 19029082]

Okada S, Aharinejad S. Lingual papillae of the growing rat as a model of vasculogenesis. Anat Rec. 1997; 247:253–260. [PubMed: 9026005]

Ozerdem U, Stallcup WB. Early contribution of pericytes to angiogenic sprouting and tube formation. Angiogenesis. 2003; 6:241–249. [PubMed: 15041800]

Patan S. Vasculogenesis and angiogenesis as mechanisms of vascular network formation, growth and remodeling. J Neurooncol. 2000; 50:1–15. [PubMed: 11245270]

Peterková R, Peterka M, Lesot H. The developing mouse dentition: a new tool for apoptosis study. Ann NY Acad Sci. 2003; 1010:453–466. [PubMed: 15033770]

Quagliata S, Pacini S, Punzi T, Malentacchi C, Ruggiero M, Delfino G. Bombesin promotes vasculogenesis and angiogenesis in chick chorio-allantoic membrane: A morphometric, structural, and ultrastructural study. J Morphol. 2008; 269:72–83. [PubMed: 17902154]

Ratajska A, Czarnowska E, Kolodzinska A, Kluzek W, Lesniak W. Vasculogenesis of the embryonic heart: origin of blood island-like structures. Anat Rec A. 2006; 288:223–232.

Ribatti D. The discovery of endothelial progenitor cells. An historical review. Leuk Res. 2007; 31:439–444. [PubMed: 17113640]

Rothová M, Feng J, Sharpe PT, Peterková R, Tucker AS. Contribution of mesoderm to the developing dental papilla. Int J Dev Biol. 2011; 55:59–64. [PubMed: 21425080]

Tertemiz F, Kayisli UA, Arici A, Demir R. Apoptosis contributes to vascular lumen formation and vascular branching in human placental vasculogenesis. Biol Reprod. 2005; 72:727–735. [PubMed: 15564598]

Trubiani O, Tripodi D, Delle Fratte T, Caputi S, Di Primio R. Human dental pulp vasculogenesis evaluated by CD34 antigen expression and morphological arrangement. J Dent Res. 2003; 82:742–747. [PubMed: 12939361]

Tsuzuki H, Sasa S. Ultrastructural observation of capillary sprouts in the dental organs of rat molars. Kaibogaku Zasshi. 1994; 69:684–696. [PubMed: 7531382]

Weihua Z, Tsan R, Schroit AJ, Fidler IJ. Apoptotic cells initiate endothelial cell sprouting via electrostatic signaling. Cancer Res. 2005; 65:11529–11535. [PubMed: 16357162]

Yuan GH, Zhang L, Zhang YD, Fan MW, Bian Z, Chen Z. Mesenchyme is responsible for tooth suppression in the mouse lower diastema. J Dent Res. 2008; 87:386–390. [PubMed: 18362325]

Zhang YD, Chen Z, Song YQ, Liu C, Chen YP. Making a tooth: growth factors, transcription factors, and stem cells. Cell Res. 2005; 15:301–316. [PubMed: 15916718]
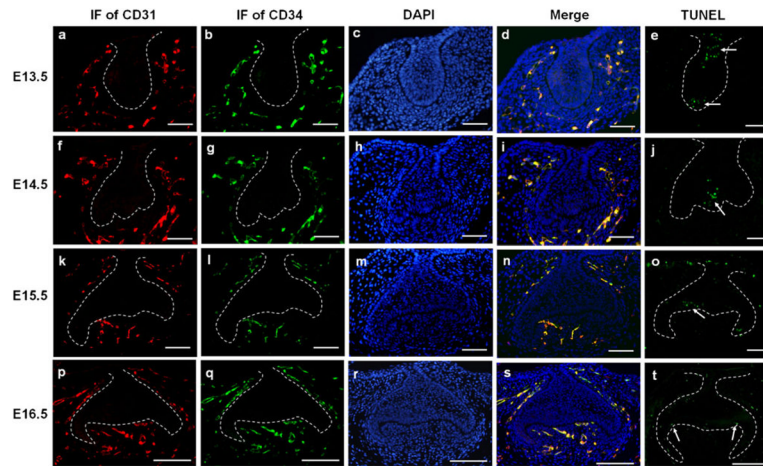
Fig. 1.
Double immunofluorescence of CD31 and CD34 and TUNEL assay in mouse molar germs from E13.5 to E16.5. **a**–**e** At E13.5, CD31-and CD34-positive cells were localized in the peripheral mesenchyme (**ad**). TUNEL-positive cells (*arrows*) were observed in the dental epithelium (**e**). **f**–**j** At E14.5, CD31- and CD34-positive cells were distributed in the dental follicle and the mandibular portion of the dental papilla (**f**–**i**). Apoptotic cells (*arrow*) were seen in the EK (**j**). **k**–**o** At E15.5, CD31-and CD34-positive cells were visualized in the central part of the dental papilla as well as in the dental follicle. Some of them were even in close proximity to the presumptive odontoblasts (**k**–**n**). Apoptotic cells were observed in the residual EK (*arrow*) and dental lamina (**o**). **p**–**t** At E16.5, in addition to the dental follicle, CD31- and CD34-positive cells were abundant in the dental papilla and organized in a regular orientation from the basal mesenchyme toward the presumed cusp positions (**p**–**s**). Apoptotic cells (*arrows*) were found in the secondary EKs (**t**). **a**, **f**, **k**, **p** Immunofluorescence of CD31; **b**, **g**, **l**, **q** immunofluorescence of CD34; **c**, **h**, **m**, **r** DAPI staining; **d**, **i**, **n**, **s** merged images; **e**, **j**, **o**, **t** TUNEL assay. *Bars* (**a**–**o**) 50 µm, (**p**–**t**) 100 µm
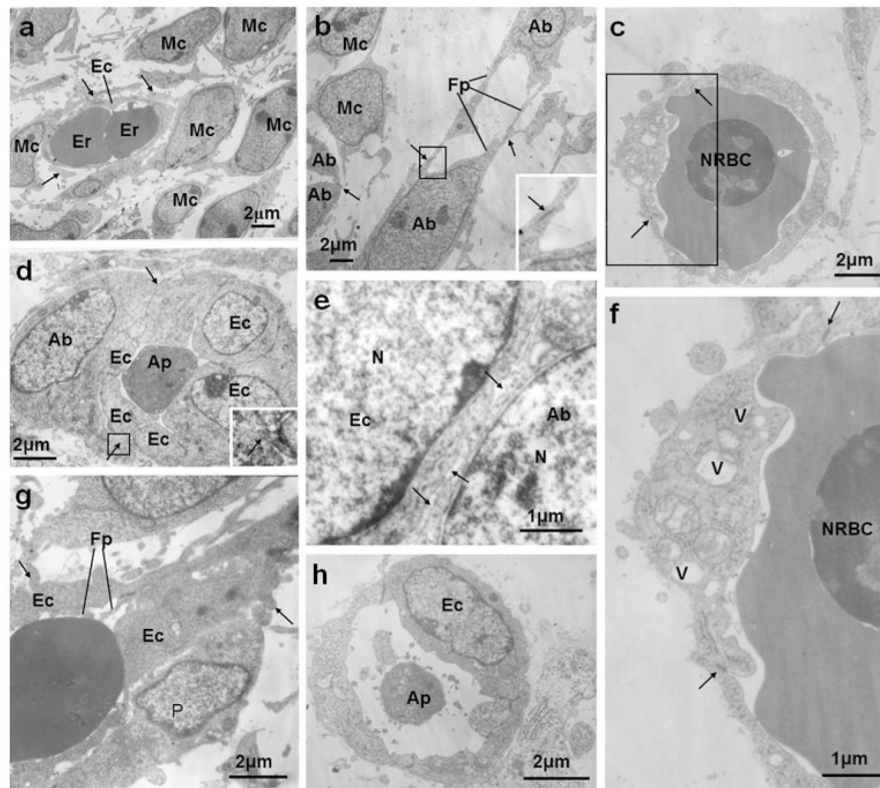
Fig. 2.
Representative electron micrographs of vasculature at E13.5 (**a**) and at E14.5 (**b–h**). **a** In
E13.5 molar mesenchyme, a newly formed capillary with an exiguous lumen was
surrounded by mesenchymal cells (*Mc*). Short cytoplasmic processes (*arrows*) from
mesenchymal cells (*Mc*) were closely opposed to or made contact with the abluminal surface
of endothelial cells (*Ec*). The ovoid mesenchymal cells (*Mc*) contained large nuclei and
scarce cytoplasm. *Er* Erythrocyte. **b** Angioblasts (*Ab*) with large nuclei interconnected
across characteristic filopodial extensions (*Fp*) were seen in the dental follicle at E14.5. The
minute junctional structures (*arrows*) between the angioblasts (*Ab*) consisted in small dense
spots on opposite plasma membranes. Higher magnification (*inset*) of the *rectangle* showed
the junction (*arrow*) between the angioblasts. **c** Presumptive endothelial cells were observed
in the dental follicle at E14.5, connected end by end (*arrows*) to each other, resulting in a
primitive vascular lumen filled with a nucleated red blood cell (NRBC). The NRBC
exhibited a halo around its nucleus. **d** An electron micrograph of an immature microvascular
tube with thick endothelium was taken in the dental follicle at E14.5. An apoptotic debris
(*Ap*) with electron-dense cytoplasm, a few recognizable degenerate mitochondria and a
collection of glycogen were located at the center of the primitive lumen. An angioblast-like
cell (*Ab*) adhered to the endothelium of the microvascular tube through filopodia extensions
(*arrows*). Higher magnification (*inset*) of the *rectangle* showed the contact between the
angioblast-like cell and the endothelial cell. **e** Small intercellular spaces (*arrows*) were
present between the neighboring endothelial cell (*Ec*) and angioblast (*Ab*). *N* nucleus. **f**
Higher magnification of the rectangle in (**c**) showing cytoplasmic vacuolar spaces (*V*) and
the minute junction structures (*arrows*) between the developing endothelial cells. **g** A
representative capillary with a lateral sprouting in which the endothelial cells (*Ec*) are rich in
filopodia (*Fp*) was visualized in the dental papilla at E14.5. Note that many cytoplasmic
protrusions (*arrows*) from the endothelium were directed toward the perivascular space. The

intercellular space between the endothelial cell (*Ec*) and pericyte-like cell (*P*) was irregular. **h** An apoptotic body (*Ap*) with electron-dense cytoplasm and well-preserved mitochondria was included in the capillary in the dental papilla at E14.5
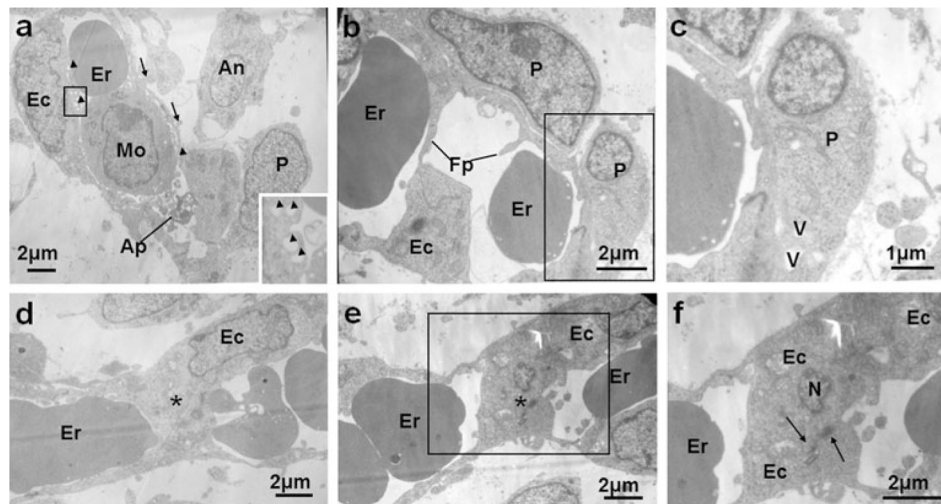
Fig. 3.
Representative electron micrographs of vasculature at E15.5 (**a**–**c**) and E16.5 (**d**–**f**). **a** A capillary in E15.5 molar mesenchyme contained an erythrocyte (*Er*), an apoptotic body (*Ap*) and a monocyte (*Mo*). Finger-like processes (*arrows*) from endothelial cells extended toward the abluminal spaces. Pinocytic vesicles (*arrowheads*) lay under the luminal cytoplasm. The basement membrane between the pericyte-like cell (*P*) and endothelium was discontinuous. Higher magnification (*inset*) of the *rectangle* showed multiple pinocytic vesicles in the cytoplasm. **b** A capillary in the molar mesenchyme at E15.5 showed cytoplasmic filopodia (*Fp*) at the luminal side rising toward the opposite side. Once the cytoplasmic filopodia (*Fp*) reached the opposite side, the pre-existing capillary was split into two vascular units. **c** Detail of the *rectangle* in (**b**) showed a pericyte-like cell (*P*) containing cytoplasmic vacuolar spaces (*V*) adhered to the abluminal surface of the capillary. **d**, **e** In the dental mesenchyme at E16.5, endothelial cell bridges (*asterisks*), including the nuclear area (**e**) or not (**d**), split the lumen of a capillary into two compartments. **f** Higher view of the *rectangle* in (**e**) showing the endothelial cell bridge connected by junctional complexes (*arrows*) separating two luminal spaces
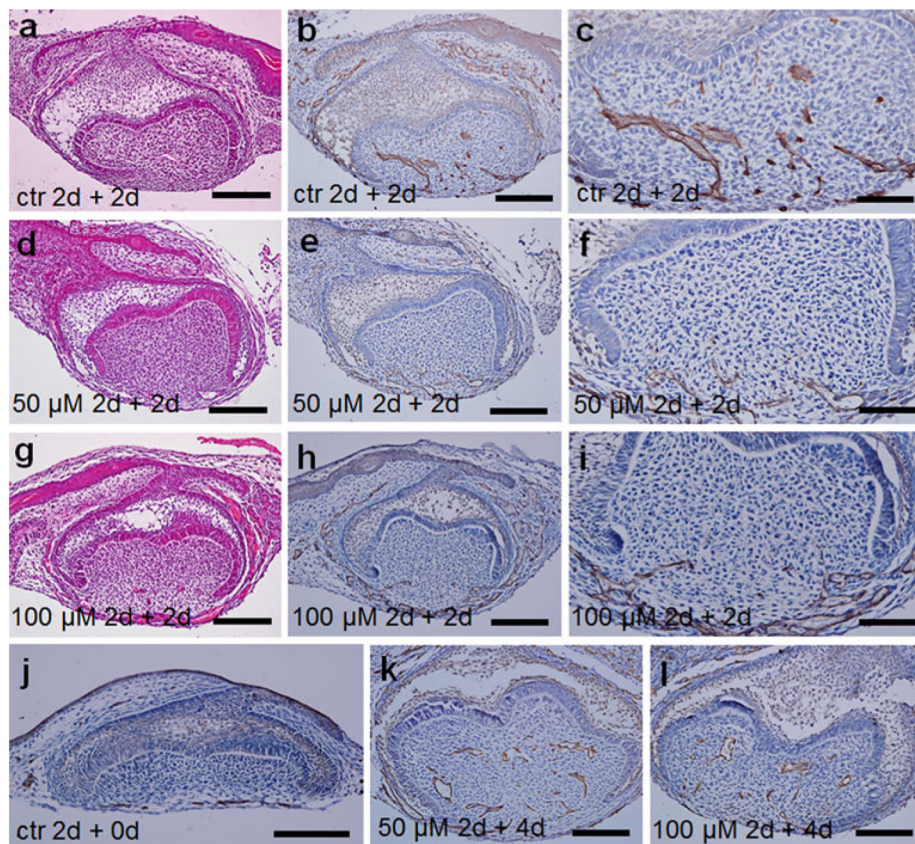
Fig. 4.
The histology, and vascularization of the mouse molar mesenchyme examined by CD31 immunohistochemistry after z-VAD-fmk treatment. E14.0 first lower molars were cultured in vitro in control medium (**a–c, j**) or in the presence of 50 (**d–f, k**) or 100 µM (**g–i, l**) z-VAD-fmk for 2 days, then cultured under mouse kidney capsules for 0 (**j**), 2 (**a–i**), or 4 days (**k, l**). **a–c** In the control molars, blood vessels appeared in the central part of the dental papilla after 2-day subrenal culture. **d–i** Blood vessels were only localized in the mandibular portion of the dental mesenchyme and the surrounding tissue in the 50-µM group (**d–f**) and in the 100-µM group (**g–i**) after 2-day subrenal culture. **j** Blood vessels are only detected in the surrounding dental follicle in the molars cultured in vitro in control medium for 2 days. **k, l** Capillaries are noted not only in the dental follicle but also in the dental papilla after a 2-day culture with the presence of z-VAD-fmk and a following 4-day subrenal culture. **a, d, g** H&E staining; **b, c, e, f, h–l** CD31 immunostaining. *Bars* (**a, b, d, e, g, h, j–l**) 100 µm, **c, f, i** 50 µm